

RECENT PROGRESS WITH EU-XFEL*

D. Reschke[#], DESY, Hamburg, Germany
for the European XFEL Accelerator Consortium

Abstract

The superconducting accelerator of the European XFEL consists of the injector part and the main linac. The injector includes one 1.3 GHz accelerator module and one 3.9 GHz third-harmonic module, while the main linac will consist of 100 accelerator modules, operating at an average design gradient of 23.6 MV/m. The fabrication and surface treatment by industry as well as RF acceptance tests of the required 808 superconducting 1.3 GHz cavities are close to an end by the time of SRF 2015. The accelerator module assembly, testing and installation in the tunnel is in full swing. First steps of commissioning have been made. The status and results of cavity and module RF tests at 1.3 GHz and 3.9 GHz are presented.

INTRODUCTION

The 17.5 GeV SRF linac for the European XFEL is currently under construction by a consortium consisting of several European institutes [1]. An enhanced cryomodule production rate of 1.25 eight-cavity-module per week since beginning of 2015 requires an average vertical acceptance testing rate and delivery of at least ten cavities per week. The average cryomodule testing rate has to match this production rate. Testing of both, individual cavities and cryomodules, is performed in a dedicated test facility at DESY (AMTF) [2,3,4,5]. As of July 31, 2015 approximately 740 of the 800 series EU-XFEL TESLA-type 1.3 GHz SRF cavities have been produced, and have each undergone at least one vertical acceptance test at AMTF. As of September 10, 2015 ~57 of the 102 EU-XFEL cryomodules (see below) have been tested at AMTF. Vertical and module testing is performed by a team from IFJ-PAN Krakow as an in-kind contribution. The installation of cryomodules and first steps of commission for the injector as well as for the main linac are in full swing.

XFEL CAVITIES AND VERTICAL ACCEPTANCE TEST AT AMTF

Production Overview

Series production of the 1.3 GHz TESLA cavities is equally divided between E. Zanon Spa. (EZ), Italy, and Research Instruments GmbH (RI), Germany. Production includes both mechanical fabrication and surface preparation [6] with the required extensive documentation [7]. Details about the RF measurements for quality assurance during the cavity production and the devices used for frequency measurement and tuning can be found in [8,9,10]. The 800 series cavities required for XFEL (400 per vendor) are delivered complete with a helium

tank, ready for vertical testing in AMTF (Fig.1) at DESY. Each vendor also produces an additional 12 cavities without helium tank for the ILC-HiGrade programme [11], which are used as a quality control tool as well as for further R&D. For 8 of these 24 cavities a subsequent assembly of the He-tank will be made. Both vendors must exactly follow well-defined specifications for the mechanical fabrication and surface treatments, but no RF performance guarantee is given. The surface preparation at both vendors starts with a bulk EP followed by 800° annealing, but for the final surface treatment two alternative recipes are in use: EZ applies a final chemical surface removal (“Flash-BCP”); RI applies a final electrochemical surface removal (EP). All cavities are fully equipped with their HOM antennas, pick-up probe and a High-Q input coupler antenna with fixed coupling. The procedures before and after the vertical acceptance test at 2K are described in [12].

At the time of SRF 2015 the mechanical cavity production is nearly finished. The tested ~740 cavities clearly demonstrate that the chosen scheme for mechanical production and surface preparation is successful at both vendors.

Due to pores out of DESY specification found in the longitudinal welds of the Helium service pipe made of Titanium about 750 He-tanks had to be modified, partially on He tanks already welded onto cavities. This major effort including the necessary qualification steps has been performed successfully over the last two years and is described in detail in [13].

Vertical Testing Rates

In order to achieve the desired testing rate of at least eight to ten cavities per week, the vertical acceptance tests are made using two independent test systems, each consisting of an independent bath cryostat and RF test stand. Each test cryostat accepts an “insert” which supports up to four cavities, greatly increasing the efficiency of cool-down / warm-up cycles. The test infrastructure at DESY (Fig.1) has been in full operation since October 2013 and has achieved a stable average of about 42 vertical tests per month (Fig. 2). All vertical acceptance tests of the 824 cavities will be finished within the current project schedule (end of 2015). Each vertical test is categorized according to well-defined “test reasons”. Depending on the result a categorized “decision” is taken and documented in the cavity and cryomodule managing system [14] of the AMTF as well as in the XFEL cavity data base [15]. Cavities without non-conformities and with acceptable performance usual have only one vertical acceptance test (“as received”) after which they receive the decision “send to string

[#]detlef.reschke@desy.de

assembly”. In case of non-conformities (e.g. insufficient cavity performance, RF problem, vacuum leak, mechanical deviation, etc.) the cavity is retested, retreated or sent back to the vendor resulting in additional vertical tests. A detailed analysis of the number and causes of conducted retests and retreatments is given in [16].



Figure 1: Preparation area for vertical testing (top) and vertical test installations (bottom) at AMTF.

The vertical acceptance tests follow a standardised procedure, which includes the measurement of the unloaded Q_0 versus the accelerating gradient E_{acc} at 2 K, as well as the frequencies of the fundamental modes. For each point of the $Q_0(E_{acc})$ -curve, X-rays are measured inside the concrete shielding above and below the cryostat. No general administrative gradient limit is applied. The average statistical measurement error is calculated to be $\sim 4\%$ for E_{acc} and $\sim 7\%$ for Q_0 [17]. In general the systematic error is about $\sim 10\%$ for E_{acc} and up to $\sim 20\%$ for Q_0 . In few cases the test-to-test comparison showed larger deviations than the above estimated errors. Within the tight production and test schedule an additional retest was performed for a small fraction of cavities for clarification, but often no obvious reason for the observed difference could be identified.

In addition to the $Q_0(E_{acc})$ curves many cavities have had the Higher Order Mode frequencies of the TE111, TM110 and TM011 modes measured [18], depending on the fabrication process.

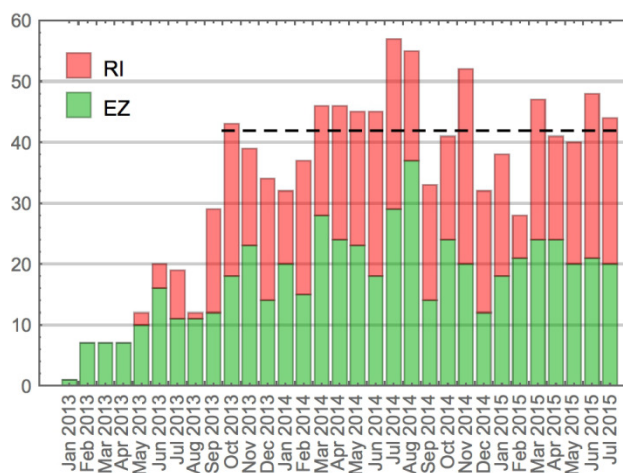


Figure 2: Trend of the vertical test rate.

After a successfully completed test, selected key data are transferred to the XFEL Cavity Data Base [15,19,20], which forms the basis of the analyses report here.

Definition of “Usable Gradient” and Acceptance Criteria

Although all cavities are tested to their maximum achievable gradient ($E_{acc,max}$), of greater importance for accelerator operation is the “Usable Gradient” ($E_{acc,us}$), which takes Q_0 as well as field-emission performance into account. It is defined as the lowest value of:

- quench gradient (quench limited);
- gradient at which Q_0 drops *below* 10^{10} (Q_0 limited);
- gradient at which either X-ray detector *exceeds* the threshold (field-emission limited).

For the field-emission limit, the acceptable X-ray thresholds are set to 0.01 mGy/min and 0.12 mGy/min for the top and bottom detector respectively. The threshold 0.01 mGy/min is based on experience from the cavity testing for FLASH. The higher limit for the lower detector is a geometrical effect.

At the beginning of production, the criterion for acceptance for module assembly was specified as $E_{acc,us} \geq 26$ MV/m, chosen to give a margin of $\sim 10\%$ compared to the required average design operation gradient (23.6 MV/m at $Q_0 \geq 10^{10}$). Based on an analysis of about 270 cavities tested up to May 2014, including the necessary retreatments and retests, the acceptance criteria was reduced to $E_{acc,us} \geq 20$ MV/m, in order to optimise the number of vertical tests while still maintaining an average module gradient of 23.6 MV/m.

Cavities with $E_{acc,us} < 20$ MV/m are considered for further processing or re-treatment. The exact nature of the handling of low-performance cavities is judged on a case by case basis. As there are no vendor performance guarantees, retreatments are in general the responsibility of DESY. Nevertheless both vendors have agreed to perform numerous retreatments depending on the case.

VERTICAL TEST RESULTS

‘As received’ from Vendor (1st Acceptance Test)

Figure 3 shows histograms and yield curves for the vertical test performance for both maximum and usable gradient, “as received” from the vendors. Compared to [17] the number of vertical acceptance is nearly doubled. The present analysis is based on 671 vertical tests (EZ: 359; RI: 312). Table 1 summarises the average of the distributions shown in Fig. 3. The average usable gradients for both vendors are above the required operational gradient for XFEL. The usable gradient is reduced from the maximum performance by 3.7 MV/m on average, predominantly due to the Q_0 -value drops below 10^{10} . The effect can be seen in Fig. 3 as an increase (top to bottom plot) in the numbers of cavities with performance less than 30 MV/m. For both vendors ~15% of the cavity tests are caused by a necessary retreatment due to field emission, which is about 5% less and a clear improvement compared to the analysis of mid 2014 [17].

There is also a statistically significant difference in the average performance of the two vendors (~4 MV/m and ~3 MV/m for the maximum and usable gradients respectively), and gradients above 40 MV/m have mainly been observed with RI cavities. The better performance is attributed to the use by RI of electropolishing as the final surface preparation scheme as described above, but also to the fact that RI cavities show less quenches at low gradients.

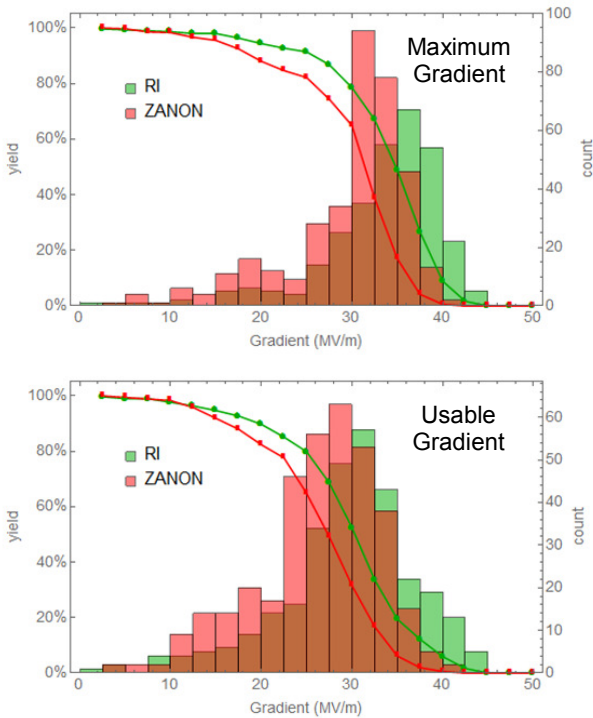


Figure 3: Comparison of performance distribution and yield for maximum gradient (top) and usable gradient (bottom) “As received” from RI (red) and EZ (green).

The percentage (“yield”) of cavities above 26 MV/m (20 MV/m) usable gradient is 59% (82%) for EZ and 75%

(90%) for RI, with a total yield of 66% (86%). All yield values are significantly increased compared to [17].

Table 1: Average (± 1 .std.dev) of the Maximum and Usable Gradient “As received”

	Tests	Maximum E_{acc} [MV/m]	Usable E_{acc} [MV/m]
Total	671	31.4 ± 7.0	27.7 ± 7.2
EZ	359	29.6 ± 6.8	26.3 ± 6.8
RI	312	33.3 ± 6.6	29.4 ± 7.4

Figure 4 shows the trend of the usable gradient “as received” referring to the arrival date at DESY together with the number of cavities tested “as received” in the respective month. Until late summer 2014 the average gradient is app. 27 MV/m, while in summer 2014 a significant improvement started resulting in an average gradient of app. 29 MV/m. The effect can be observed for both vendors, but with a different time pattern and is finally more pronounced for EZ. As the overall procedures and specifications for surface treatment remained unchanged, the positive effect can be explained by retraining combined with an enhanced experience of the cleanroom staff. For summer 2015 a downward trend is observed, which is currently under investigation with the vendors.

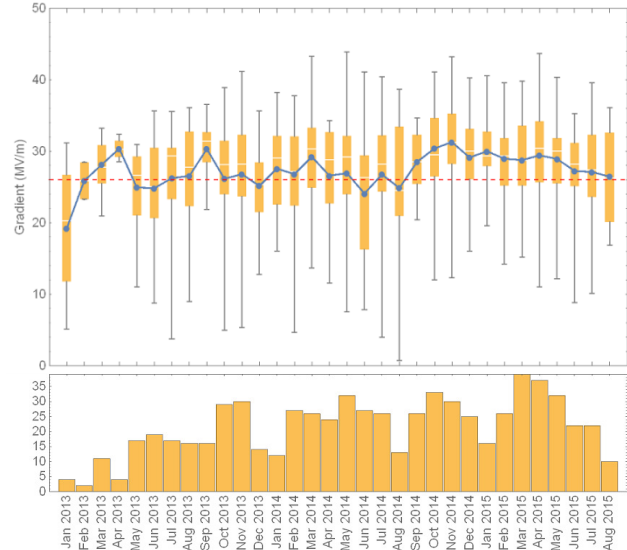


Figure 4: Trend of the usable gradient “As received” (top) with the number of tested cavities “As received” (bottom).

Impact of “Retreatment”

As described above, most cavities with usable gradients below 20 MV/m undergo re-treatment with a goal of increasing their performance. Often a high resolution optical inspection is performed before the retreatment in order to localize the limiting defect [21]. As a consequence of the improved cavity quality delivered from both vendors in the last year the number of necessary retreatments due to bad performance has been

reduced. Based on the current statistics approximately 17% of all cavities have been retreated and retested due to insufficient performance. In general, high-pressure ultra-pure water rinsing (HPR) is applied as a first retreatment. This is particular effective since most low-performance cavities are dominated by field emission, which is likely associated with a removable surface emitter (e.g. particles). More details are reported in [22, 23].

CRYOMODULE TEST RESULTS

The string and module assembly at CEA Saclay is described in [24]. An actual status, improvements, recent results and correlations are presented in [25,26]. So far more than 60 modules have been assembled with a nominal rate of one cryomodule per week, first achieved in October 2014. In Jan 2015 the assembly rate could be enhanced to 1.25 per week. In order to match the accelerated cryomodule assembly, the test procedures with respect to mechanical, vacuum, cryogenic and RF aspects have been improved and optimized [4,5]. With these improvements test durations below 15 days have been achieved provided that no significant non-conformities (e.g. cryogenic or vacuum leaks, power coupler components) appear.



Figure 5: Cryomodules (top) and cryomodule test stand installations (bottom) at AMTF.

So far 57 cryomodules have been RF tested at the AMTF (Fig. 5). This includes the pre-series modules XM-1 and XM-2, which are equipped with EU-XFEL series

cavities. The cryomodule XM-3 is not included as its cavities are of FLASH type and a tunnel installation is not foreseen due to missing PED certification.

Comparability of “Usable and Operational Gradient” in vertical vs. cryomodule test

The definition of the usable gradient in the vertical test (VT) has been given above, and is based on limits Q_0 and x-ray performance.

Comparing these criteria to the RF measurement conditions in the cryomodule test (CT) stand it becomes obvious that no simple 1 : 1 correlation of gradients of individual cavities is possible.

- The RF power limits are not comparable: In the VT a maximum power of $\sim 200\text{W}$ (“long-pulse” quasi cw) is applied. The resulting gradient depends on Q_0 of the cavity as well as on the external Q -value of the input antenna. In the CT the maximum RF power (limited by average power at used RF circulator) is about 220 kW for 10Hz operation limiting all gradients at 31 MV/m.
- In the CT no Q_0 -value for individual cavities can be measured. The time consuming heat load measurement is done for all eight cavities together at one (typically 20 – 23.6 MV/m) gradient (an additional measurement at 15 MV/m was skipped with the optimization of test procedures due its large error and in order to gain more time at higher gradient).
- Radiation values are taken in both VT and CT, but with different geometrical locations of the radiation sensors. Therefore no direct comparison is possible, even if all handling and string assembly procedures keep the field emission behaviour exactly unchanged.
- As a result of the above points, only the thermal breakdown (“quench”) gradient – if below 31 MV/m – is a comparable figure of merit.

Table 2: Comparison of Mean Value (± 1 .std.dev) for Maximum and Operational Gradient for all Cavities assembled to rf tested Cryomodules. IMPORTANT: For Comparability the VT Gradients are clipped to the CT Limit of 31 MV/m before averaging.

	Tests	Maximum E_{acc} [MV/m]	Operational E_{acc} [MV/m]
VT	431	30.4 ± 1.7	28.9 ± 2.5
CT	431	28.4 ± 4.1	27.2 ± 4.6

“Maximum gradient” in CT vs. VT

Figure 6 shows the maximum achieved CT gradients for all individual tested cavities in comparison to their VT test results. The dashed red line gives the above explained RF power limit in the CT at 31 MV/m. In an ideal case all results should scatter around a line with a slope = 1. Obviously a number of cavities show a reduced

performance in the CT after a good to excellent behaviour in the VT (lower right section of the plot). The third column of Table 2 gives the means for the maximum gradients for the VR and CT respectively. More details and possible correlations of the performance to non-conformities during the overall module assembly process are given in [25].

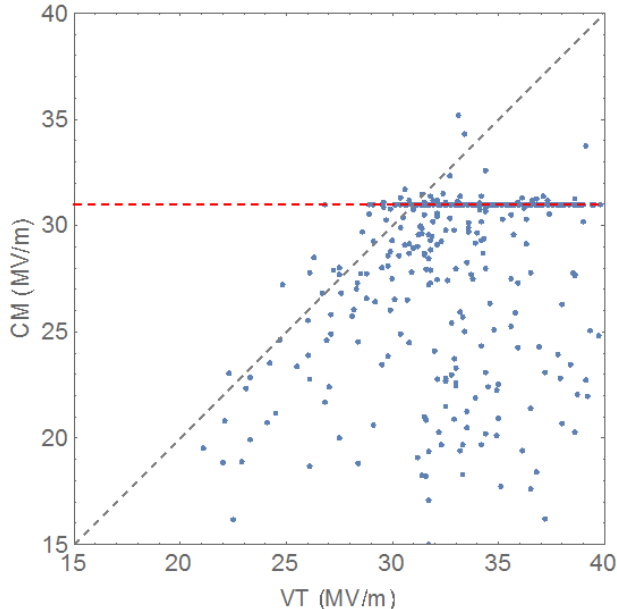


Figure 6: Individual CT – VT comparison for the maximum gradient. The horizontal red dashed line is the power limit in the CT (note some early tested were allowed to exceed this value).

“Usable / Operational Gradient” in CT vs. VT

In Fig. 7 the average operational gradients for all cryomodules tested so far are presented and compared to the respective average vertical test results. For a suitable comparison all vertical test gradients above 31 MV/m are clipped before averaging. Table 2 shows the mean operational gradients over all cryomodules with the CT gradient meeting the VT gradients within 7%.

Except for XM26 the order of assembly is in agreement with ascending cryomodule numbering. An average gradient loss can be observed in about the first half of assembled cryomodules, which then improved significantly for more recently assembled modules. This is due to improvements in the cleanroom procedures and additional operator trainings, which are described in detail in [25, 27]. XM33, XM45 and XM58 show the lowest performance. As XM33 and XM58 are equipped with cavities showing VT gradients of 22 MV/m and 23 MV/m, respectively, no higher gradients can be expected in CT. The strong degradation of XM45 can be correlated with an accidental loss of electricity in the cleanroom during string assembly.

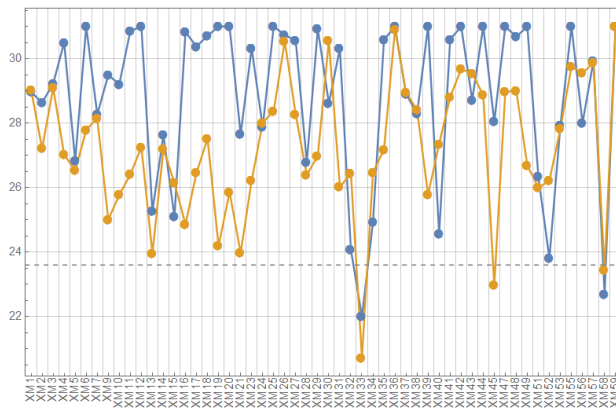


Figure 7: Average cryomodule operational gradients (orange) compared to the respective average vertical test results (blue). IMPORTANT: For comparability the VT gradients are clipped to the CT limit of 31 MV/m before averaging.

Quality Factor at Operational Gradient in CT vs. VT

The dynamic cryogenic heat load at 2K of a module is dominated by the Q_0 -values (i.e. their surface resistance) of the cavities at their operational gradient. Figure 8 shows the CT effective average Q_0 -values at (20 – 23.6) MV/m calculated from the cryo losses in comparison to the expected average Q_0 -values from the vertical tests. As a main result all cryomodules except of XM34 meet the EU-XFEL design goal of $\geq 1 \cdot 10^{10}$. The mean Q_0 -value for CT is about $1.4 \cdot 10^{10}$ and very close to the VT Q_0 -value of $1.3 \cdot 10^{10}$. Exceptions to significantly higher CT Q_0 -values are either caused by an enhanced measurement error at low heat loads due to a poor “signal to background” ratio or may be caused by a dependence of the RF losses on the cooldown procedure [28].

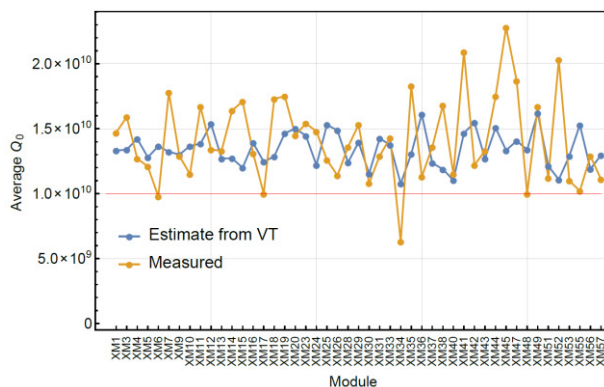


Figure 8: Average cryomodule Q_0 -values measured by cryogenic heat load measurement at an operational gradient of (20-23)MV/m.

INJECTOR

The EU-XFEL injector consists of a 43m long beamline and uses the same L-Band photocathode RF-gun design

which is also serving as the electron source for the FLASH Linac at DESY and the “photo injector test facility” PITS in Zeuthen [29]. The normal conducting gun is driven by an RF-station identical to the ones used for the SC-1.3GHz RF-modules. The momentum of the electrons reaches up to 6 MeV/c within the gun before they enter the first SC-module (Fig. 9), which is one of the standard XFEL modules and will increase the momentum to about 130 MeV/c. In addition there is the superconducting 3rd harmonic module to manipulate the longitudinal phase space of the bunches. The main purpose is to improve the compression of the bunches in order to reach the bunch length and high peak current necessary to start the SASE process.

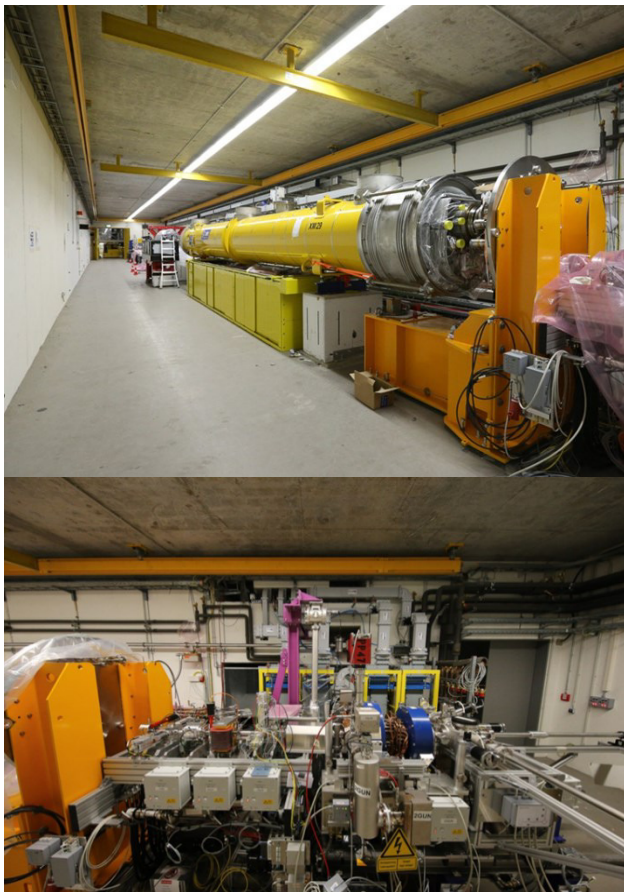


Figure 9: 1.3GHz injector module (top) and photocathode RF gun (bottom) in the XFEL injector building.

The second half of the injector allows the measurement of all relevant beam parameters. At the end a dipole can be used to send the beam into a local dump, which allows the stand alone operation of the injector while the installation of the main linac proceeds.

As the last major component the 3rd-harmonic module will be installed from September to November 2015. The cool-down of the modules and the start of the injector commissioning is foreseen for November 2015.

THE EU-XFEL 3RD HARMONIC SYSTEM

The third harmonic system at 3.9 GHz of the EU-XFEL injector section is a joint INFN and DESY contribution and consists of a single module hosting eight SRF cavities and a quadrupole magnet package. The module design was derived from the FLASH third harmonic section, developed by FNAL [30], with some major modifications in the module and cavity package design, in particular the development of a cavity string with alternate coupler orientation with respect to the beamline [31], for coupler dipole kick compensation [32].

Cavity Production and VT Qualification

The procurement of a set of ten 3.9 GHz cavities started in 2012, after the experience with three prototypes used to set the industrial production and treatment steps. The necessary conformance of the design and fabrication procedures to the European Pressure Equipment Directive (PED) norms had significant influence on the production schedule [33]. As a consequence the first eight cavities fully qualified in the INFN Vertical Testing facility reached DESY ready for string assembly in the period from December 2014 to March 2015, and the last two at the end of May 2015. All the cavities were tested exceeding specification, represented by the EU-XFEL icon in Fig. 10, reaching at least 18 MV/m with Q_0 above 10^9 at this field level. None of the cavities showed field emission. Nearly all cavities are quench limited. Although a few of the tests were limited by available RF power [34].

In addition ten more fully equipped cavities are presently under fabrication for a spare cryomodule.

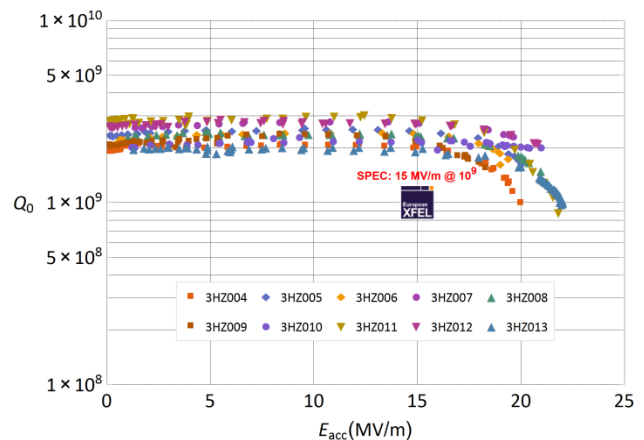


Figure 10: Summary plots for $Q_0(E_{acc})$ of the ten 3.9 GHz cavities at 2 K.

Power Coupler and Cavity Package

The 3.9GHz power couplers are of the same FNAL design used in FLASH, but with the antenna length adapted to the different EU-XFEL beam structure. They were industrially procured and processed after fabrication at FNAL. The eight couplers necessary for the string installation were sent in pairs in their conditioning boxes

from FNAL and were available at DESY from mid-February to Mid-June 2015.

In contrast to the 1.3GHz cryomodules no full cold test of the 3.9 GHz module at AMTF will be done, but the module will be commissioned and characterized in the injector after installation. This decision is based on the moderate performances needed by the 3.9 GHz cavities as well as on infrastructure and schedule constraints. Therefore the successful system test of one “cavity package” in March 2015 consisting of a horizontal cavity equipped with power coupler, tuner and wave guide tuners represented an important verification before the module assembly [35].

X3M1 Module Assembly and Installation

Though the 3.9 GHz module assembly consists essentially of the same operations needed for the 1.3 GHz modules, some small deviations were needed for several reasons: different cavity and ancillary components like tuner and couplers, tighter spaces - the module is only 6 m long but hosts the same number of smaller active components - and increased diagnostics (a large number of temperature sensors has been placed on the cavity string to detect possible temperature increases at the cavity HOM regions during beam operation, due to the smaller cavity aperture).

The module assembly was performed in summer 2015 [36] and had an overall duration of 14 weeks, from the availability of the eight cavities with installed couplers to the injector installation. Figure 11 shows the module ready for tunnel installation.



Figure 11: The 3.9 GHz harmonic module during its final preparation stages before installation in the E-XFEL injector tunnel.

CRYMODULE INSTALLATION AND COMMISSIONING

Cryomodule Installation

The EU-XFEL cold linac cryogenic layout is shown in Fig. 12. The main linac is divided in 3 sections L1, L2 and L3. Between the sections there are 2 warm bunch compressors (BC1 and BC2), where the cryogenic connection requires 2 transfer lines. The sections are composed as:

- L1 (CS1) with 4 cryomodules, one feed (FC) and one end cap (EC).
- L2 (CS2) with 12 cryomodules, one feed and one end cap.
- L3 (CS3-9) with 12 cryomodules each divided by string connection boxes (SCB).

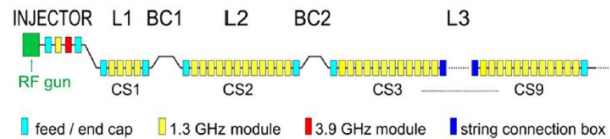


Figure 12: Layout of the EU-XFEL linac.

All the cryogenic pipes contained in the cryomodules, FCs, ECs, and SCBs are connected together by welding in order to reduce the risk of leaks introduced by flanged connections. Each connection is made of 2 or 3 welds, since a bellow is installed between the 2 pipe ends protruding from the modules, caps or boxes (Fig. 13). Special welding tools and processes have been developed to reach the required quality levels for the safe operation of the EU-XFEL cryogenic components for the next 20 years, while dealing with tight space requirements and schedule. The non-destructive tests of each weld, necessary for the approval of the linac as a pressure equipment include 100% visual test, 100% radiography test and 100% leak test and require special developed tools.

At each connection a beam line absorber for HOM damping is mounted on the beam line with flanged connections. A portable, dedicated clean room has been developed to allow a reproducible and reliable UHV connection effectively reducing the risk of particulate contaminations of the beam line vacuum.



Figure 13: A typical module-module connection, where only the gas return pipe and 2-phase line are positioned for the first weld operations.

More details about the cryogenic layout, the cryo and beam line absorber installation work can be found in [37]. The installation progress for cryomodules and key components is shown in Fig. 14.

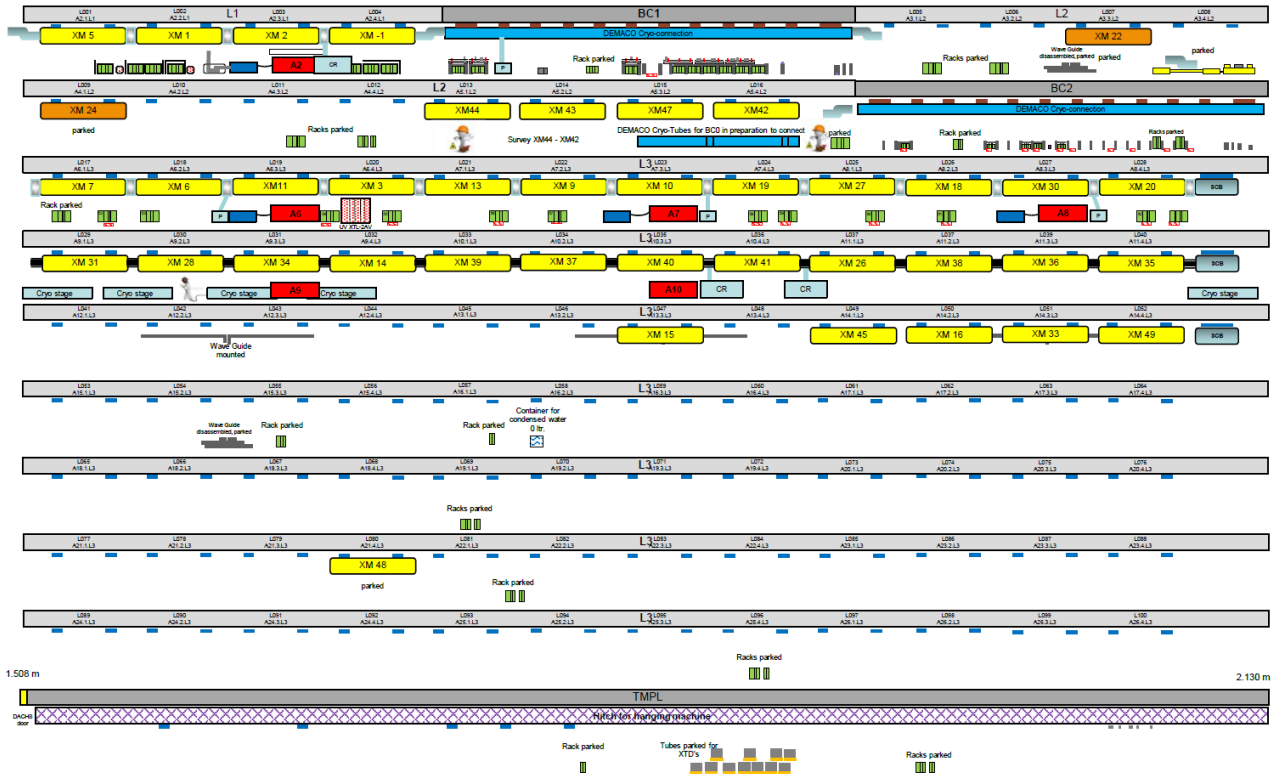


Figure 14: Installation progress of cryomodules and important components to the EU-XFEL tunnel as of Sep 18, 2015.

New RF Power Coupler Interlock and Warm RF Commissioning

The safe operation of cavities during commissioning and beam operation is secured by a new technical interlock (TIL) design [38] (Fig. 15), which is based on the XFEL crate standard (MTCA™.4). The new interlock is located inside the accelerator tunnel. Several remote test capabilities ensure the correct operation of sensors for light, temperature and free electrons. Due to the space costs and the very high number of channels, the electronic concept was moved from a conservative, mostly analog electronic approach, with real comparators and thresholds, to a concept, where the digitizing of the signals is done at a very early stage. Filters, thresholds and comparators are moved into the digital part. The usage of a Field Programmable Gate Array (FPGA), an additional watchdog and a modular hardware concept increase the flexibility dramatically in order to be as reliable as possible.

The default RF Station contains one klystron and a low level RF system, four cryomodules and one TIL system (Table 3). The TIL system is split in two parts (master and slave), each for 16 cavities and couplers. Compared to the slave, the master contains additionally the cryo and vacuum channels and is generating the overall alarm sum for the RF station.

During the start-up and warm commissioning of the first RF station operating on four cryomodules with 144 fast and 72 slow sensor channels, beside several

diagnostic channels the TIL system proved its full functionality as well as robust EMC design.

Table 3: Interlock Signals for one RF Station

Count	Signal	Remark
96	e ⁻ sensor	Current meas. with bias voltage
32	Spark	Air side (waveguide) of main coupler
64	PT1000	Ceramic RF window (T70K, T300K)
12	analog	IGP vacuum and high voltage
2	analog	Cryo signals (He level; pressure)
1	contact	Vacuum system status
1	RS422	Cryo system status



Figure 15: Micro TCA™ Rear Transition Module.

SUMMARY

The accelerator cavity production and treatment at both vendors is close to be finished and highly successful. The 1.3GHz cryomodule assembly at CEA Saclay, testing at AMTF as well as cryo and vacuum installation to the EU-XFEL is in full swing. The 3.9 GHz third harmonic system is ready for injector installation and cold commissioning before end of 2015. The first warm commissioning of a four cryomodule RF station applying a new developed technical interlock system for the power coupler proved its functionality. Scheduled date for the closing of the main linac tunnel is June 30, 2016, followed by the cool-down.

ACKNOWLEDGMENT

The European XFEL cavity and cryomodule fabrication, testing and installation is a collaborative effort of several European institutes and their industrial partners. The author likes to thank the complete team of all involved institutes for their work and support.

REFERENCES

- [1] "The European X-Ray Free-Electron Laser; Technical Design Report", DESY 2006-097 (2007), <http://www.xfel.eu/documents>
- [2] Y. Bozhko et al., "Cryogenics of European XFEL Accelerator Module Test Facility", Proc. ICEC 23, Wroclaw 2011, p.911
- [3] J. Swierblewski, "Large Scale Testing of SRF Cavities and Modules", TUIOC01, Proc of the LINAC 2014, Geneva, Switzerland
- [4] J. Swierblewski et al., "Improvements of the mechanical, vacuum and cryogenic procedures for European XFEL Cryomodule Testing", TUPB115, these proceedings, SRF2015, Whistler, Canada (2015)
- [5] M. Wiencek et al., "Improvements of the RF test procedure for European XFEL Cryomodule testing", TUPB118, these proceedings, SRF2015, Whistler, Canada (2015)
- [6] W. Singer et al., "The Challenge and Realization of the Cavity Production and Treatment in Industry for the European XFEL", MOIOA03, Proc. Conf. on RF Superconductivity 2013, Paris, France (2013)
- [7] J. Iversen et al., "Release processes and Documentation Methods during Series Treatment of SRF Cavities for the European XFEL by using Engineering data Management System", THPB032, these proceedings, SRF2015, Whistler, Canada (2015)
- [8] A.Sulimov, "RF measurements for Quality Assurance during SC Cavity Mass Production", WEBA02, these proceedings, SRF2015, Whistler, Canada (2015)
- [9] A. Sulimov, "RF Analysis of Equator Welding Instabilities for E-XFEL Cavities", THPB066, these proceedings, SRF2015, Whistler, Canada (2015)
- [10] J.-H. Thie et al., "Operation Experience with half Cell Measurement machine & Cavity Tuning Machine in 3 years of XFEL series Production", THPB031, these proceedings, SRF2015, Whistler, Canada (2015)
- [11] A. Navitski et al., "ILC-HiGrade Cavities as a Tool of Quality Control for European XFEL", MOP043, Proc. Conf. on RF Superconductivity 2013, Paris, France (2013)
- [12] D. Reschke, "Infrastructure, Methods and Test Results for the Testing of 800 Series Cavities for the European XFEL", THIOA01, Proc. Conf. on RF Superconductivity 2013, Paris, France (2013)
- [13] A. Matheisen et al., "Exchange and Repair of Titanium Service Pipes for the EXFEL Series Cavities", THPB025, these proceedings, SRF2015, Whistler, Canada (2015)
- [14] M. Wiencek et al., "Cavities and Cryomodules managing system at AMTF", TUPB117, these proceedings, SRF2015, Whistler, Canada (2015)
- [15] S. Yasar et al., "A Database for the European XFEL", MOP041, Proc. Conf. on RF Superconductivity 2013, Paris, France (2013)
- [16] J. Schaffran et al., "Analysis of test rate for European XFEL series cavities", MOPB079, these proceedings, SRF2015, Whistler, Canada (2015)
- [17] D. Reschke et al., "Analysis of the RF Test Results from the On-going Cavity Production for the European XFEL", THPP021, Proc of the LINAC 2014, Geneva, Switzerland
- [18] A. Sulimov et al., "Practical Aspects of HOM Damping Changes for TM011 of the E-XFEL Cavities", THPB068, these proceedings, SRF2015, Whistler, Canada (2015)
- [19] S. Yasar et al., "European XFEL database structure and data loading system for cavities and modules", THPB038, these proceedings, SRF2015, Whistler, Canada (2015)
- [20] S. Yasar et al., "User interfaces applied for the European XFEL data base for cavities and modules", THPB039, these proceedings, SRF2015, Whistler, Canada (2015)
- [21] A. Navitski et al., "Characterisation of surface defects on E-XFEL series and ILC-HiGrade cavities", MOPB072, these proceedings, SRF2015, Whistler, Canada (2015)
- [22] N.J. Walker et al., "Update and status of vertical test results of the XFEL series cavities", MOPB086, these proceedings, SRF2015, Whistler, Canada (2015)
- [23] A. Matheisen et al., "Experiences on Retreatment of XFEL Series Cavities at DESY", MOPB075, these proceedings, SRF2015, Whistler, Canada (2015)
- [24] C. Madec et al., "The Challenge to Assemble 100 Cryomodules for the European XFEL", THIOA02, Proc. Conf. on RF Superconductivity 2013, Paris, France (2013)

- [25] O. Napoly, "Module performance in XFEL cryomodule mass production", FRAA02, these proceedings, SRF2015, Whistler, Canada (2015)
- [26] M. Wiencek et al., "Update and status of the test results of the XFEL series accelerator modules", MOPB080, these proceedings, SRF2015, Whistler, Canada (2015)
- [27] S. Berry et al., "Cleanliness and vacuum acceptance tests for the UHV cavity string of the XFEL linac", MOPB118, these proceedings, SRF2015, Whistler, Canada (2015)
- [28] Various presentations about the influence of the cool down parameters on the Q_0 -value at these conference, SRF2015, Whistler, Canada (2015)
- [29] B. Dwersteg et al., "RF gun design for the TESLA VUV free electron laser", NIM A393, p.93-95 (1997)
- [30] E. Harms et al., "Commissioning and early operating experience of the FLASH third harmonic system", TUP013, proc.LINAC10, p.422 (2010)
- [31] P. Pierini et al., "Preparation of the 3.9 GHz System for the European XFEL Injector Commissioning", TUPB018, these proceedings, SRF2015, Whistler, Canada (2015)
- [32] E. Vogel et al., "Considerations on the third harmonic RF of the European XFEL", WEP07, proc.of SRF2007, Beijing (2007)
- [33] P. Pierini et al., "Fabrication of the 3.9 GHz SRF Structures for the European XFEL", THPB035, these proceedings, SRF2015, Whistler, Canada (2015)
- [34] D. Sertore et al., "Vertical Tests of XFEL 3rd Harmonic Cavities", MOPB077, these proceedings, SRF2015, Whistler, Canada (2015)
- [35] C. Maiano et al., "Horizontal RF Test of a Fully Equipped 3.9 GHz Cavity for the European XFEL in the DESY AMTF", MOPB076, these proceedings, SRF2015, Whistler, Canada (2015)
- [36] M. Schmökel et al., "Assembly of a 3.9GHz String for the E-XFEL at DESY", TUPB0105, these proceedings, SRF2015, Whistler, Canada (2015)
- [37] S. Barbanotti et al., "Connection of EU-XFEL Cryomodules, Caps and Boxes in the EU-XFEL Main Linac and Injector: Welding of Cryo-pipes and Assembly of Beam-line Absorbers under the Requirements of the PED Regulation", TUPB108, these proceedings, SRF2015, Whistler, Canada (2015)
- [38] D. Tischhauser et al., "Next Generation Cavity and Coupler Interlock for the European XFEL", THPB080, these proceedings, SRF2015, Whistler, Canada (2015)